Performance assessment of evapotranspiration estimated from different data sources over agricultural landscape in Northern India

[1]Prashant K. Srivastava, [1]Prachi Singh, [1]R.K. Mall, [1,2]Rajani K. Pradhan,

[3]Michaela Bray, [4]Akhilesh Gupta

[1]DST-Mahamana Centre for Excellence in Climate Change Research, Institute of Environment and Sustainable Development, Banaras Hindu University, Varanasi-221005, UP

[2]Faculty of Environmental Sciences, Czech University of Life Sciences Prague, Czech Republic

[3]University of Cardiff, Wales, UK

[4]Department of Science and Technology, New Delhi, Government of India

Correspondence: rkmall@bhu.ac.in

Abstract: Accurate estimation of evapotranspiration is generally constrained due to lack of required hydro-meteorological datasets. This study addresses the performance analysis of Reference Evapotranspiration (ETo) estimated from NASA/POWER, National Center for Environmental Prediction (NCEP) global reanalysis data before and after dynamical downscaling through the Weather Research and Forecasting (WRF) model. The state of the art Hamon's and Penman-Monteith methods were utilized for the ETo estimation in the Northern India. The performances indices such as Bias, Root Mean Square Error (RMSE) and correlation(r) were calculated, which showed the values 0.242, 0.422 and 0.959 for NCEP data (without downscaling) and 0.230, 0.402,0.969 for the downscaled data respectively. The results indicated that after WRF downscaling, there was some marginal improvement found in the ETo as compared to the without downscaling datasets. However, a better performance was found in the case of NASA/POWER datasets with Bias, RMSE and correlation values of 0.154 0.348 and 0.960 respectively. In overall, the results indicated that the NASA/POWER and WRF downscaled data can be used for ETo estimation, especially in the ungauged areas. However, NASA/POWER is recommended as the ETo calculations are less complicated than those required with NASA/POWER and WRF.

Keywords: Evapotranspiration; Hydrology; WRF model; Seasonality; NCEP

1. Introduction

Evapotranspiration defined as the "combined loss of water from a given area, and during a specified period of time by evaporation from the soil surface and by transpiration from plants" (Thornthwaite 1948). It is considered as one of the most important components of the hydrological cycle (Mall and Gupta 2002; Srivastava et al. 2016). On the Earth surface, it has very important role in the context of water and energy balances as well as required in the irrigation and agriculture practices (Nag et al. 2014). In addition, evapotranspiration is required in many scientific disciplines to understand the underlying hydrological processes (Petropoulos et al. 2015; Petropoulos et al. 2016). However, in spite of the several efforts made by many government agencies, there are still lack of sufficient meteorological stations for measurement of reliable and accurate datasets for ETo estimation.

Previously, indirect approaches are generally used for ETo measurements (Srivastava et al. 2017). One means of estimating ETo is through the use of a Lysimeter which determines the evapotranspiration by recording the amount of precipitation an area receives and how much is lost through the soil. However due to high maintenance cost, time consumption and lack of precise instrumentation, its implementation is not easy, especially for larger areas (Pandey et al. 2016). Nevertheless there are a number of other methods developed in past decades which quantify ETo (Alkaeed et al. 2006; Djaman et al. 2015; Lang et al. 2017). Among them, the simplest approach was developed by Hamon (Hamon 1960), which requires only temperature data for ETo calculation. In (2015), McCabe et al. used the monthly calibrated coefficient values to calculate the ETo and found that the mean monthly ETo (using Hamon's method) were close to the mean monthly free-water surface evaporation.

From many studies, the FAO-56 Penman Monteith (PM) method is considered to be the most suitable indirect method for estimation of reference Evapotranspiration (ETo). Cai et al in (2007) used the daily real-time ETo in the field of water resources management. They found that by using the public daily weather forecast messages to calculate ETo predictions to be an appropriate method for real-time water allocation and irrigation management. Kar et al in (2016) compared the ETo, computed by eight different methods for the dry sub-humid agro-ecological region. They found that the estimated ETo calculated via the Penman-Monteith method to be a better estimate of ETo compared to all the other methods. However, a major drawback of the PM method is that it demands several meteorological parameters (wind speed, humidity, sunshine hour etc), which may not be often available everywhere (Chen et al. 2005), due to the lack of availability of stations or missing values due to station poor maintenance (Pandey et al. 2016).

There were very few studies focused on the ETo estimation using the mesoscale model like MM5 (Mesoscale modelling system 5), Weather Research and Forecasting model combined with NASA/POWER datasets etc. Some studies reported on the use of mesoscale models for estimation of ETo in different parts of the world (Falk et al. 2014; Lin et al. 2018; Srivastava et al. 2016; Srivastava et al. 2013). (Ishak et al. 2010) has estimated the ETo over Brue catchment, southwestern England using the ECMWF ERA-40 reanalysis downscaled data through MM5 model. (Silva et al. 2010) has investigated the potential use of numerical weather forecast obtained from MM5, as a proxy for surface meteorological data with specific objective to use it in the estimation of ETo over Maipo river basin. Later, (Srivastava et al. 2013; Srivastava et al. 2016) used the WRF model to downscale the ECMWF and NCEP reanalyzed datasets over the Brue catchment and reported a better performance of ECMWF than NCEP downscaled datasets.

Despite the high importance of ETo in the field of hydrology and climatological studies, there are only a few studies available in the technical literature domain, which demonstrate the accuracy and performance of the ETo derived from the WRF model and NASA/POWER datasets, especially for the Indian regions. Therefore, this paper provides a detailed cross comparison of ETo estimated from different existing datasets--NCEP, WRF downscaled NCEP and NASA/POWER over cropland by using the Hamon's and Penman Monteith's methods in the Northern India. Further detailed analysis with respect to seasonality is also provided to determine the appropriateness of these methods of deriving ETo with regards to seasonal variability. The outcomes of the study can be used by the agricultural, meteorological and hydrological departments to improve their forecast ability.

2. Materials and methodology

2.1. Study area

The study area consists of agricultural landscape, geographically lies between 25° 14' 54.94"N to 25 °17' 06.57" N and 82°58'30" E to 83°00' 35" E in the Northern India , considered as food bowl of the country. Topographically, it is located on higher ground with mean elevation of 80.71 m (Cai et al. 2009). Being situated in the Indo-Gangetic plain, the land is composed of very fertile alluvial soil deposited by Rivers Ganga and Varuna. Climatically the area is Sub humid type, characterized by hot summer, cold season and pleasant monsoon. The temperature varies from 22° C to 46° C in summer and may drop below 5°C in winter season. June is the hottest month with the mean temperature around 35° C and mid-December to January is the coldest month (<5 °C).

The mean annual rainfall is 1036 mm whereas, about 90% of the total rainfall takes place in monsoon season from June to September. Geologically the study area is characterized by Gangetic alluvium formed by the deposition sediment by river Ganga and its tributaries. The observational temperature dataset (2009-2016) is used for the estimation of ETo provided by Department of Agriculture, Banaras Hindu University, India. In addition, three sets of reanalyzed data sets--NCEP, WRF downscaled NCEP (hereafter WRF-NCEP) and NASA-POWER were collected and used for the estimation of ETo for the time period 2009-2016 and compared with the observed ETo. An overview of the methodology used in present study is shown in Figure 1.

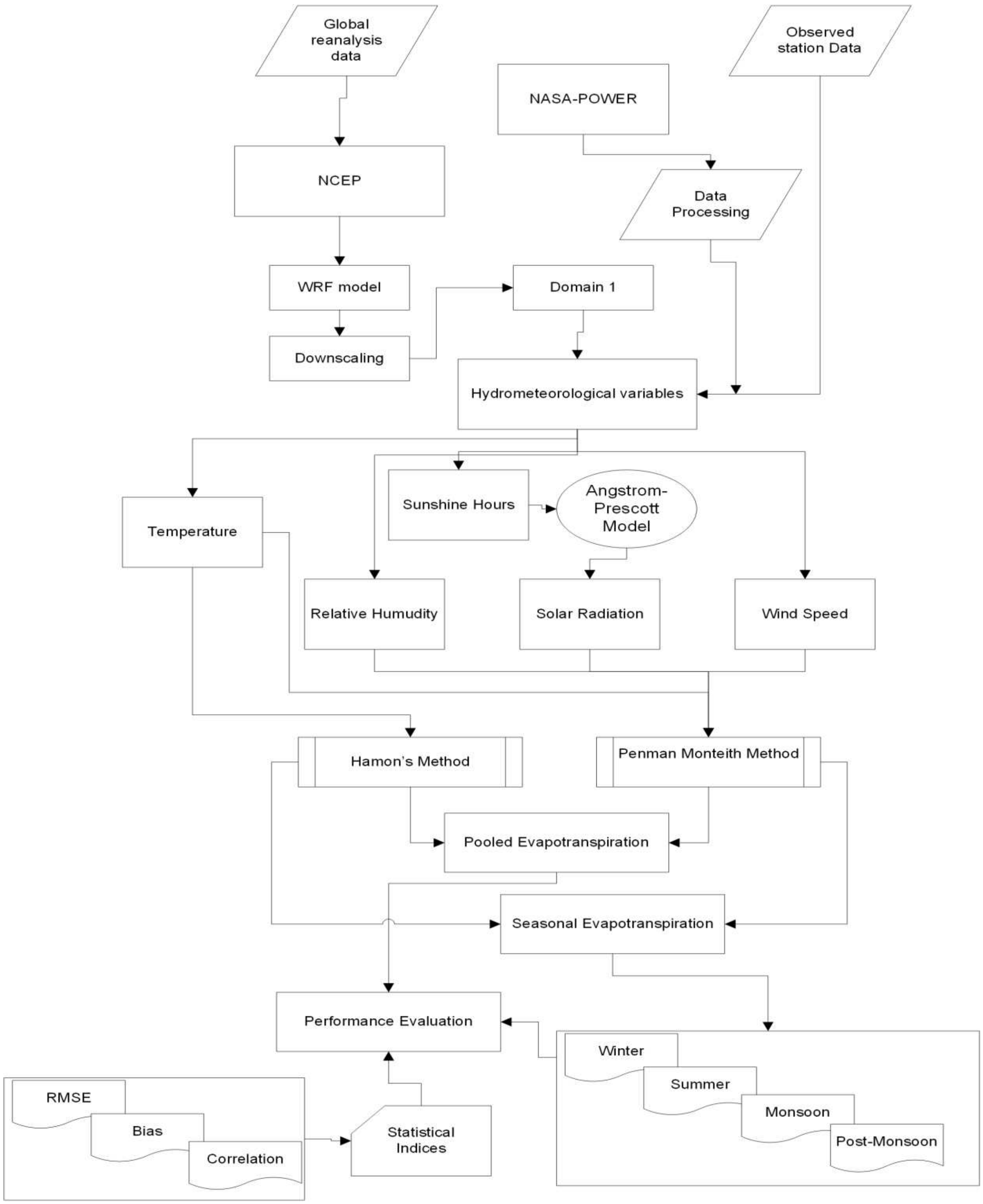

Figure.1 Flowchart of the methodology

2.2. Weather Research and Forecasting model

The WRF model was developed by scientists at the National Center for Atmospheric Research (NCAR), National Centers for Environmental Prediction (NCEP), the National Oceanic and Atmospheric Administration (NOAA), the Naval Research Laboratory, the Earth System Research Laboratory, the University of Oklahoma, the U.S. Air Force, and the Federal Aviation Administration (FAA). . The Weather Research Forecasting (WRF) is a next- generation, non-hydrostatic and mesoscale modelling system. This numerical weather prediction model and data assimilation system are used in atmospheric research and operational application (Skamarock et al. 2001). WRFI is useful for various applications such as assimilation of meteorological datasets, air quality modelling, downscaling climate simulations as well as the atmosphere research (Mohan and Sati 2016). It comprises of ARW (Advance Research WRF) and NMM (Non- Hydrostatic Mesoscale model) cores (Schwartz et al. 2009; Srivastava et al. 2016). In this study, WRF is used to downscale the NCEP data over the selected region in Northern India. Meteorological data downscaled from the WRF model was used for calculation of ETo. Derived ETo is compared with the observed dataset obtained from the station. For microphysics, we used WSM 6 - class graupel scheme inbuilt with ice, snow and graupel processes. The Graupel scheme is highly suitable for high- resolution simulations and developed at the National Center for Atmospheric Research (NCAR) (Hong and Lim 2006). The long-wave radiation RRTM (Rapid Radiative Transfer Model) scheme is used because of its high efficiency (Mlawer et al. 1997). The Dudhia scheme is used as it is efficient for cloud and clear-sky absorption and scattering (Dudhia 1988). In surface layer option, Monin-Obukhov similarity scheme is used. YSU scheme is selected to constitute near surface weather operations (Kim and Wang 2011).

2.3 NASA/POWER and NCEP datasets

In this study, the hydrometeorological variables were estimated using the NCEP data directly, after downscaling of NCEP using WRF (WRF-NCEP), NASA/POWER as well as from ground-based station. The Worldwide Energy Resources (NASA/POWER) project was initiated in 2003, which is an upgrade to the Surface meteorology and Solar Energy (SSE) project. The NASA/POWER Release-8 provides the meteorological data on a global grid scale with spatial resolution of $0.5° \times 0.5°$. The NASA/POWER data was developed by using the satellite, ground observation, windsondes, modeling and data assimilation techniques. The Meteorological data sets are taken from NASA Modern Era Retro-Analysis for Research and Applications (MERRA-2) assimilation model and from Goddard Earth Observing System Model, version 5.12.4 (GEOS) assimilation model. GEOS is a system of models integrated using the Earth System Modeling Framework (ESMF) being developed in the GMAO (Global Modeling and Assimilation Office) to support NASA's earth science research in data analysis, climate and weather prediction and basic research. In this study, the meteorological variables were downloaded from the NASA/POWER website (**https://power.larc.nasa.gov/**) for the time span of 2009-2016. In addition, the global NCEP FNL (Final) reanalysis dataset from 2009 to 2016 were used for the estimation of ETo. The NCEP-NCAR global reanalysis data set is an assimilated dataset developed using a state of art analysis forecast system (Kalnay et al. 1996). The NCEP datasets with $1^{\circ} \times 1^{\circ}$ grids are available at every 6h and can be downloaded from the website **(http://rda.ucar.edu/).** The NCEP data is available from 1948 to present and updated continuously.

2.4. Evapotranspiration estimation

2.4.1 Hamon's method

In this study, Potential Evapotranspiration (PET) is calculated using the Hamon's equation. Hamon equation uses only the temperature and is a simple and robust method for calculating Evapotranspiration (McCabe et al. 2015). PET is calculated using downscaled and non-downscaled NCEP reanalysis data and compared with the observed ETo. As the area under consideration is cropland and there is adequate availability of water, the ETo values can be considered closer to the PET values.

Hamon equation can be expressed as follows:

$$PET = K * 0.165 * 216.7 * N * \left(\frac{e_s}{T + 273.3} \right) \tag{1}$$

where PET is in (mm day^{-1}); K is the proportionality coefficient; N is the daytime length (x/12 hours); e_s is the saturation vapor pressure (hPa) and T is the average monthly temperature.

$$e_s = 6.108_e \left(\frac{17.27T}{T + 273.3} \right) \tag{2}$$

2.4.2 Penman-Monteith method

The Food and Agricultural Organization-56 (FAO) Penman-Monteith method was considered to estimate daily ETo (Monteith 1965; Penman 1956). The FAO-56 PM method is recommended as the best method for ETo estimation for all types of climates (Allen et al. 1998) and the equation for estimation of daily ETo can be expressed as:

$$ETo = \frac{0.408\Delta(R_n - G) + \gamma \frac{900}{T + 273} u_2 (e_s - e_a)}{\Delta + \gamma(1 + 0.34 u_2)} \tag{3}$$

where ETo rate is in (mm d^{-1}), R_n is net radiation at the crop surface (MJ m^{-2} day^{-1}), T= mean air temperature (ºC), u_2= wind speed (m s^{-1}) at 2 meter above the ground, e_s is saturation vapour pressure [kPa], e_a is actual vapour pressure, e_s-e_a is saturation vapour pressure deficit [kPa], Δ is slope vapour pressure curve [kPa °C^{-1}], γ is psychrometric constant [kPa °C^{-1}) and G is soil heat flux density[MJ m^{-2} day^{-1}].

$$\Delta = \frac{4098\left[0.6108 \exp\left(\frac{17.27T}{T + 237.3}\right)\right]}{(T + 237.3)^2} \tag{4}$$

where T= air temperature, e = 2.7183 (base of natural logarithm).

For the calculation of R_n (net radiation), R_a (extraterrestrial radiation) value is required. R_a can be calculated using the equation.

$$R_a = \frac{24(60)}{\pi} G_{sc} d_r [(\omega_s \sin\varphi \sin\delta) + (\cos\varphi \cos\delta \sin\omega_s)] \tag{5}$$

where R_a extraterrestrial radiation [MJ m-2 day-1], G_{sc} solar constant = 0.0820 MJ m-2 min-1, d_r inverse relative distance Earth-Sun, w_s sunset hour angle [radian], j = latitude [radian] , d = solar decimation [radian] (Zotarelli et al. 2010).

2.5 Angstrom-Prescott Model

Since, solar radiation is not available for the study area, to avoid this difficulty the FAO56 suggested Angstrom-Prescott (AP) equation, which is a simple straightforward method to predict the daily global solar radiation and therefore considered here to calculate the monthly daily extraterrestrial radiation (Podder et al. 2014). The equation is given as follows:

$$H_0 = \frac{24}{\pi} G_{sc} \left(1 + \cos\frac{360n}{365}\right) \times \left(\cos\varphi\cos\delta\sin\omega_s + \frac{\pi\,\omega_s}{180^\circ}\sin\varphi\sin\delta\right) \quad (6)$$

where H_0= solar radiation, G_{sc} solar constant (1.361 kW/m^2), n= daily maximum sunshine duration in hour, φ =latitude in degree, δ=solar declination in degree, ω_s = sunset hour angle in degree.

3. Results & Discussion

3.1. Evaluation of Hydro-meteorological variables

From NCEP, WRF-NCEP and NASA/POWER data sets, weather variables were extracted for ETo estimation. Temporal variations of temperature are shown in **Figure 2**, while combined (pooled) performance statistics are shown in **Figure 3**. The three statistical indices correlation (r), RMSE and Bias are calculated between NCEP, WRF-NCEP and NASA/POWER estimated temperature and compared with the ground-based observations. As shown in the Figure 3, we can observe a gradual increment in the temperature data, when proceeding from the winter to summer seasons. Among three datasets the WRF-NCEP data has the highest correlation (r = 0.976), followed by NCEP (r = 0.971) and NASA/POWER (0.969), which indicates a close agreement of temperature with ground observations. However, in terms of RMSE and Bias the NASA/POWER has shown a better performance followed by WRF-NCEP and NCEP estimated temperatures (Table.1). Some outliers can be seen figure 3, a detailed investigation revealed that during those days sporadic rainfall occur in the area, which is well captured by the meteorological station but not detected in any of the simulated products. These scattered or isolated rainfall in the summer season, caused a sudden cooling down of the land surface and leads to lowering of the temperature during those days. Other localized factors such as irrigation practices at specific intervals in the area, also caused a reduction in the temperature, but not detected in the global reanalysis products used in this study. These sharp variations are not properly captured by NASA/POWER, NCEP, WRF-NCEP, and thus an overestimation can be seen in the Figure 3. Further, **Figure 4** showed the performance of estimated temperature on a seasonal basis and with observed dataset. From the figure 2, temperature estimated from different sources showed a close agreement with the ground-based observations. In winter, in terms of correlation the NCEP temperature (0.948) has shown a good performance as compared to the WRF-NCEP (0.940) and NASA/POWER (0.934) datasets.

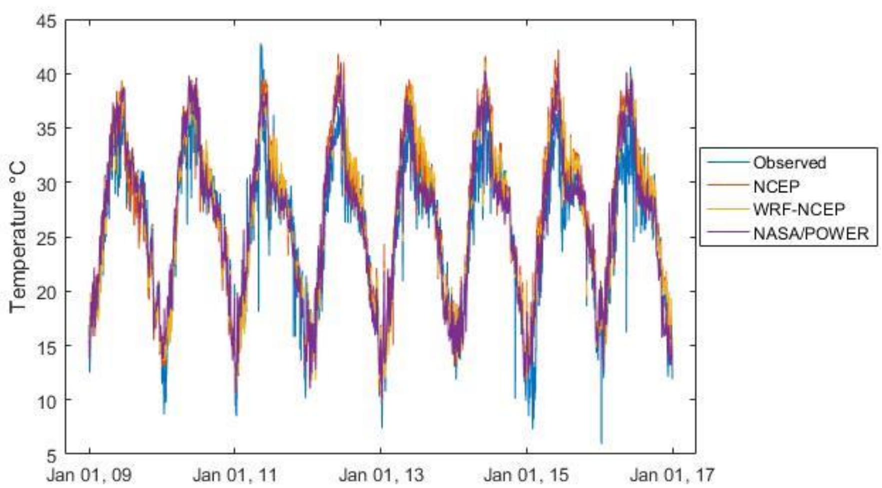

Figure 2. Temporal plot for WRF-NCEP, NCEP, NASA/POWER daily temperature with observed datasets.

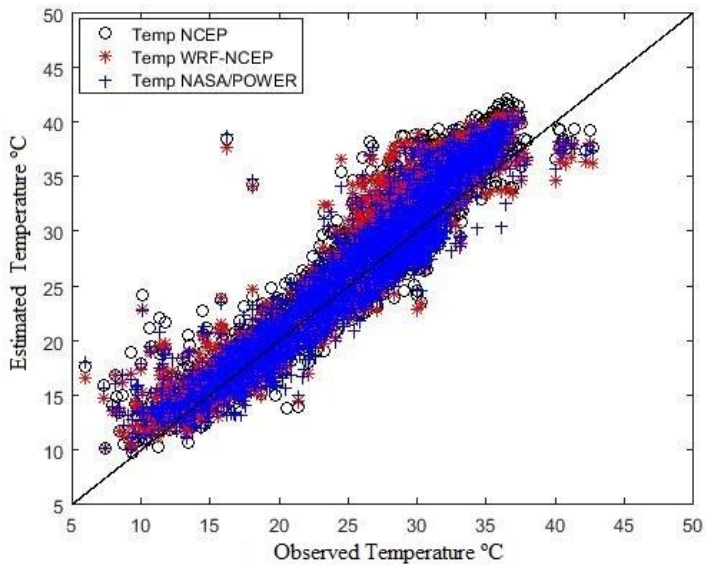

Figure 3. Scatter plot representing the variations among WRF-NCEP, NCEP and NASA/POWER temperature with observed datasets.

However, in terms of Bias and RMSE the WRF-NCEP downscaled temperature reveals better results than the other datasets. As compared to winter, in summer the estimated temperature is overestimating most of the time. Interestingly in summer, the NASA/POWER estimated temperature has the highest correlation (r=0.966) followed by WRF-NCEP (r=0.957) and NCEP (0.930). In the WRF-NCEP estimated temperature a comparatively smaller RMSE and Bias were obtained then the other datasets. During the monsoon periods, a poor performance was observed in estimated temperature especially in the WRF-NCEP and NCEP compared to the observations, while the NASA/POWER showed a better result. The frequent and abrupt changes in the weather variables in monsoon season due to rainfall, especially in the Indian continents could be one of the reasons for the poor performance of estimated temperature in the monsoon season. Finally, the post monsoon season reflects a better performance in terms of both *r* and Bias when compared to the summer and monsoon periods. Overall, in winter and summer the WRF-NCEP has shown the best results followed by NCEP and NASA/POWER, however in monsoon and post-monsoon seasons, NASA/POWER has a much better performance as compared to the WRF-NCEP and NCEP datasets.

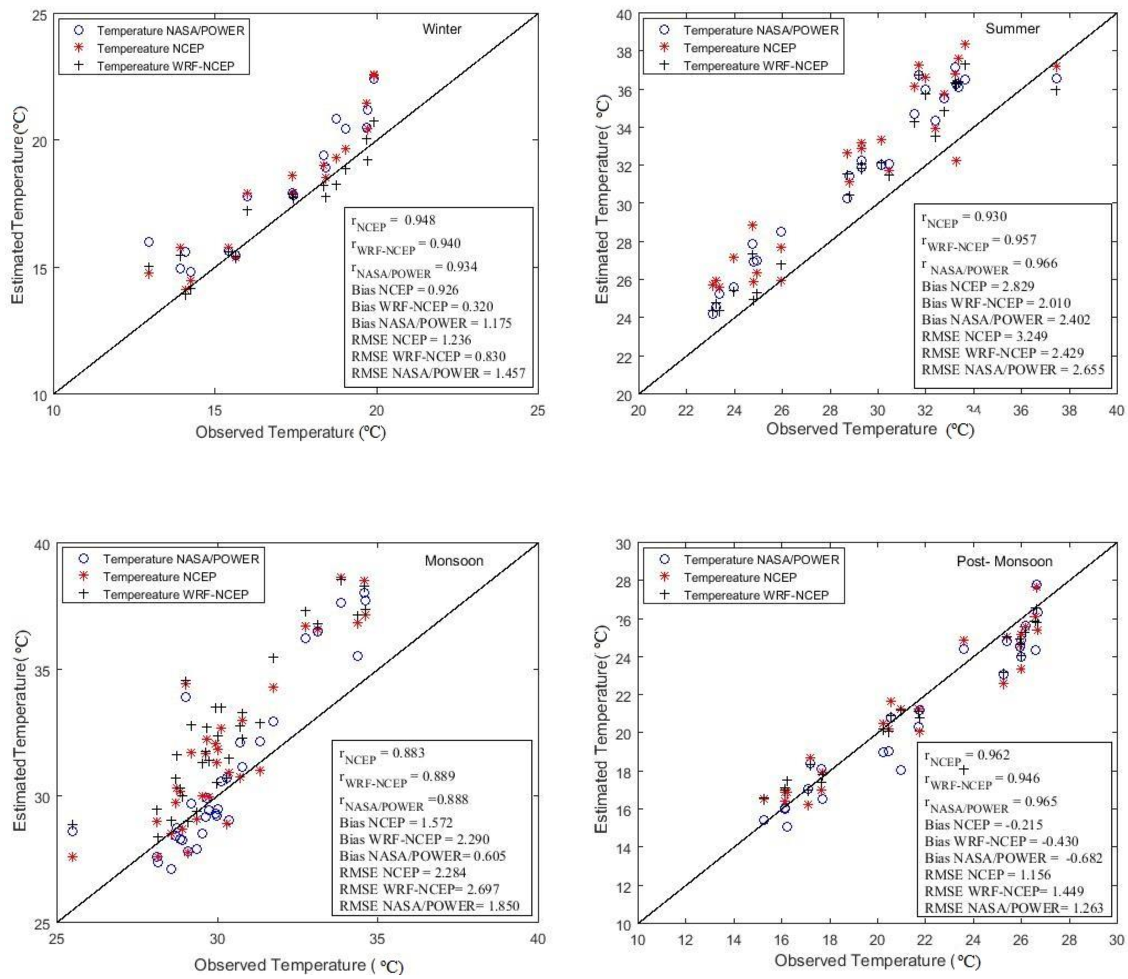

Figure 4. Scatter plot representing the seasonal variations in temperature estimated from NCEP, WRF-NCEP, NASA/POWER and observed data.

The seasonal analysis of temperature over the study area is shown in **Figure.5**. The box and whisker diagrams are used to show the overall distribution of the datasets. The main advantage of the box and whisker plot is that it represents the distribution of data in terms of maximum, minimum, median and both the upper and lower quartile in a single plot. The line cross across the box represents the median, while the whisker of the box showed the range of the given data sets. The winter WRF-NCEP downscaled data shows a close agreement with the observed temperature, while the NCEP and NASA/POWER show an overestimation. During the monsoon season NASA/POWER has a good agreement with the observed median temperature. Outside this period it is the WRF-NCEP data is in closer agreement to the observations.

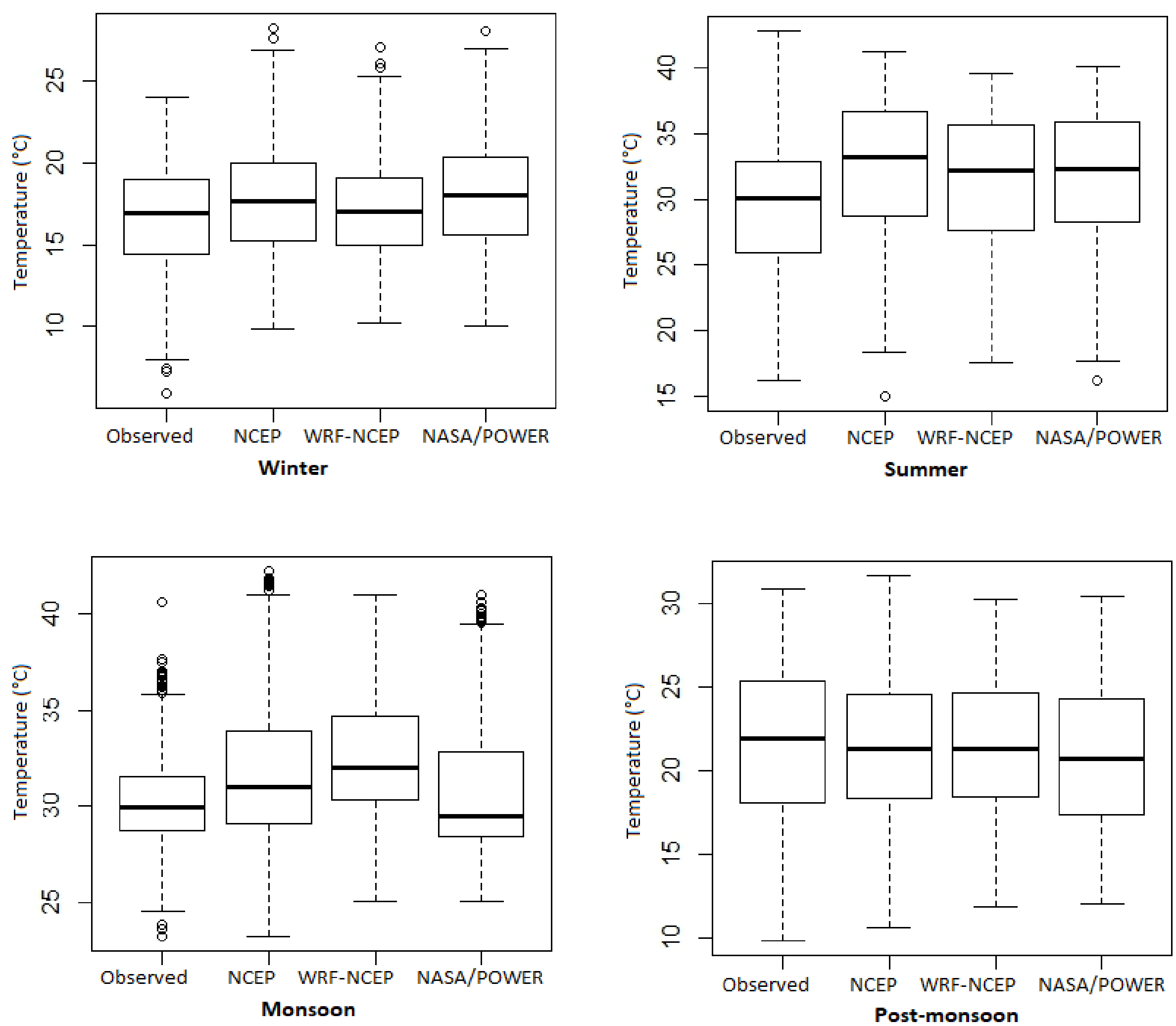

Figure 5. Seasonal distribution of temperature over the study area.

Table 1. Performance statistics of the seasonal and pooled daily temperature

Variables	NCEP			WRF-NCEP			NASA/POWER		
	r	*RMSE*	*Bias*	*r*	*RMSE*	*Bias*	*r*	*RMSE*	*Bias*
Pooled Temperature	0.971	2.233	1.333	0.976	2.134	1.210	0.969	1.914	0.826
Winter Temperature	0.948	1.236	0.926	0.940	0.830	0.320	0.934	1.457	1.175
Summer Temperature	0.930	3.249	2.829	0.957	2.429	2.010	0.966	2.655	2.402
Monsoon Temperature	0.883	2.284	1.572	0.807	2.697	2.290	0.888	1.850	0.605
Post- Monsoon Temperature	0.962	1.156	-0.215	0.947	1.449	-0.430	0.965	1.263	-0.682

3.2. Comparative assessment of evapotranspiration products

To understand the performance statistics of NCEP, WRF-NCEP and NASA/POWER estimated ETo over the study area, the relative plot of the pooled dataset with the observed ETo is shown in the **Figure. 6**. Results indicated that the NCEP and NASA/POWER data showed an overestimation most of the time. Higher ETo was observed for April to July months, this is due to the very high temperature in these months. According to correlation statistics, the WRF-NCEP has a marginal high correlation of 0.969 followed by NASA/POWER and NCEP with *r* value of 0.960 and 0.959 respectively. On the other hand, a high bias has been observed in the case of NCEP (0.241) followed by WRF-NCEP (0.230), and least in the case of NASA/POWER data (0.154). Even in terms of RMSE, as compared to the NCEP (0.422) and WRF-NCEP (0.402), the NASA/POWER showed a better performance with a value of 0.348. Both NCEP and WRF-NCEP estimated ETo showed an overestimation when compared with the ground data, whereas in case of NASA/POWER it is underestimating most of the time. Overall, the NASA/POWER data showed a small discrepancy in estimation of ETo **(Figure 7)**.

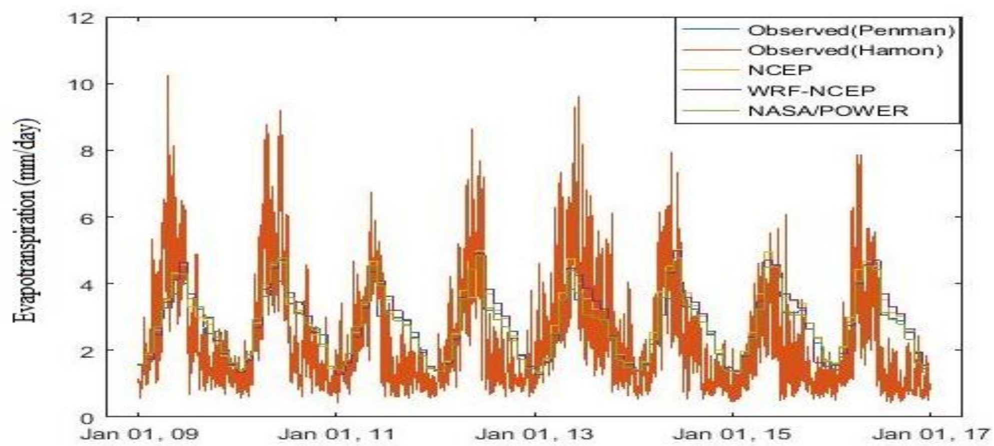

Figure 6: Temporal plots representing the variations among NCEP, WRF-NCEP and NASA/POWER daily ETo (estimated using Hamon's method) with observed data

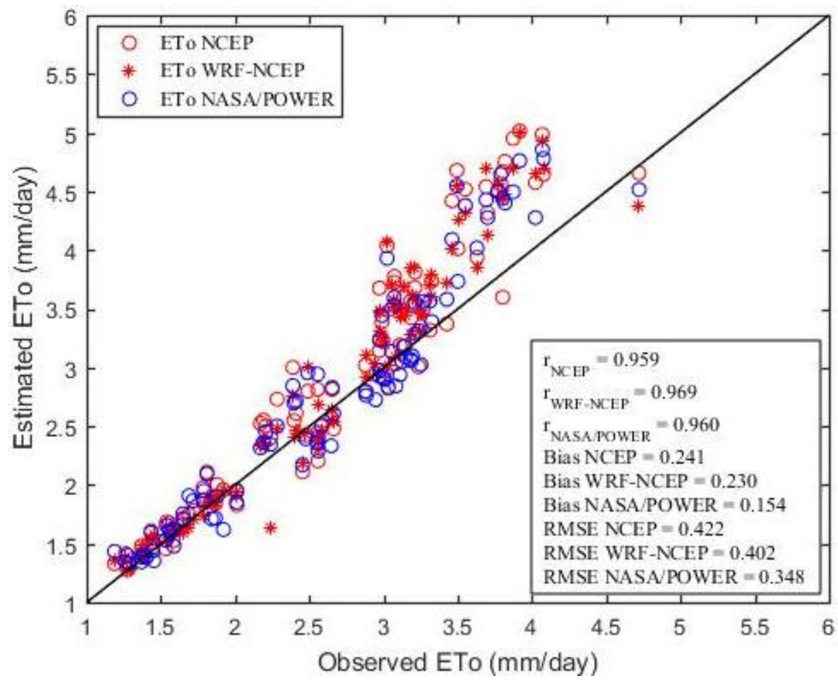

Figure 7. Scatter plots of NCEP, WRF-NCEP and NASA/POWER daily ETo with observed data

3.4 Seasonality assessment of ETo

The seasonal distribution of ETo were explained using the Box-whisker plots as shown in **Figure.8**. As it can observed from the figures, in comparison to the other datasets, the WRF-NCEP showed a good performance with the observed ETo. Further among the four seasons, the post-monsoon season (October, November and December) has less variations as compared to the observed data. In the summer and monsoon seasons, the ETo is generally over-estimating, while in case of post monsoon it shows an underestimation. In post-monsoon the WRF-NCEP analyzed data showed a good agreement with the observational data. Even though the overall results are good, the output indicated poor simulation of higher ETo values throughout the period under consideration, whereas the simulation of lower ETo values are reasonably good. In the Hamon's method, as temperature is the prime factor for the ETo calculation, the differences in the ETo value could be due to the poor quality of the temperature datasets.

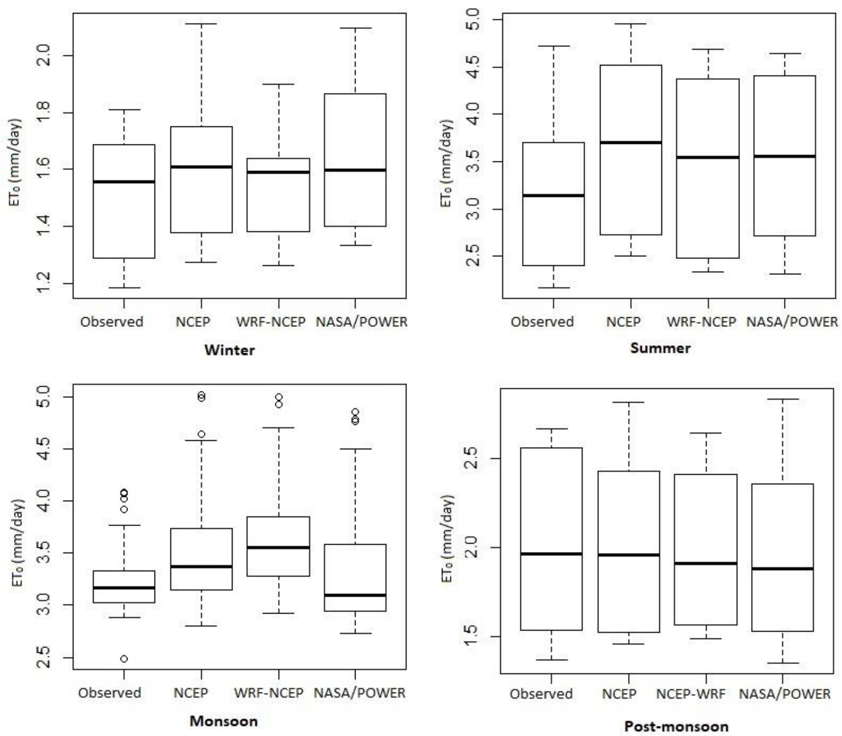

Figure 8. Seasonal distribution of ETo over the study area.

The scatter plot representing the seasonal variations in ETo derived from NCEP, WRF-NCEP, NASA/POWER and observed datasets is shown in Figure 9. The performance statistics are also calculated for the seasonal ETo and presented in Table 2. A considerable difference was found between the NASA/POWER, NCEP and WRF-NCEP for all the four seasons. For the winter season, the values of *r, Bias and RMSE* were reported as 0.945, 0.089 and 0.121 for NCEP respectively, while for WRF-NCEP the values of *r*=0.947, *Bias*=0.026 and *RMSE*=0.070 were obtained. On the other hand, for NASA/POWER, values of 0.940, 0.112 and 0.139 respectively were obtained for *r, Bias and RMSE* respectively. The results in the winter season indicated that the WRF-NCEP is performing better than the other dataset in this season. In the summer season *r, Bias and RMSE* were found as 0.908, 0.523 and 0.628 for NCEP respectively, while the WRF-NCEP revealed values of 0.936, 0.373 and 0.480 for *r, Bias and RMSE* respectively. Similarly, for NASA/POWER, the values of *r*=0.949, *Bias*=0.439 and *RMSE*=0.511 were obtained, which indicated that the WRF-NCEP can simulate a better ETo than the NASA/POWER and NCEP datasets. For monsoon season *r, Bias and RMSE* (in the order) were reported as 0.896, 0.311 and 0.461 for NCEP, 0.902, 0.442 and 0.535 for WRF-NCEP and 0.904, 0.136 and 0.373 for NASA/POWER estimated ETo respectively. Analysis revealed that during the Monsoon season, NASA/POWER was found much better than the other datasets for ETo estimation. For post-monsoon season *r, Bias and RMSE* were reported as (in the order) 0.956, -0.034 and 0.143 for NCEP, 0.949, -0.063 and 0.167 for WRF-NCEP, 0.960, -0.081 and 0.153 for NASA/POWER data respectively. The results indicated that the during post-monsoon season there is no improvement after downscaling or by using the NASA/POWER dataset as NCEP itself is giving better performance than the other two datasets. This indicate that a better parametrization scheme or combination of different parametrization schemes are needed in WRF for simulation of temperature during post-monsoon season. In the seasonal analysis, for summer and winter seasons, the WRF-NCEP estimated ETo yields a lower RMSE than the NCEP and NASA/POWER data and show a very close agreement with the observed dataset. However, due to better capture of physics especially by WRF during monsoon season, a more accurate ETo simulation was obtained, as a high performance was obtained in the pooled dataset. The results indicated that as the performances of WRF-NCEP and NASA/POWER based ETo are very close, therefore, any of them can be used for the ETo estimation. However, as WRF-NCEP requires high performance computing facility and based on complex physics, NASA/POWER could be a better choice for different applications, as it can be directly obtained from the provider.

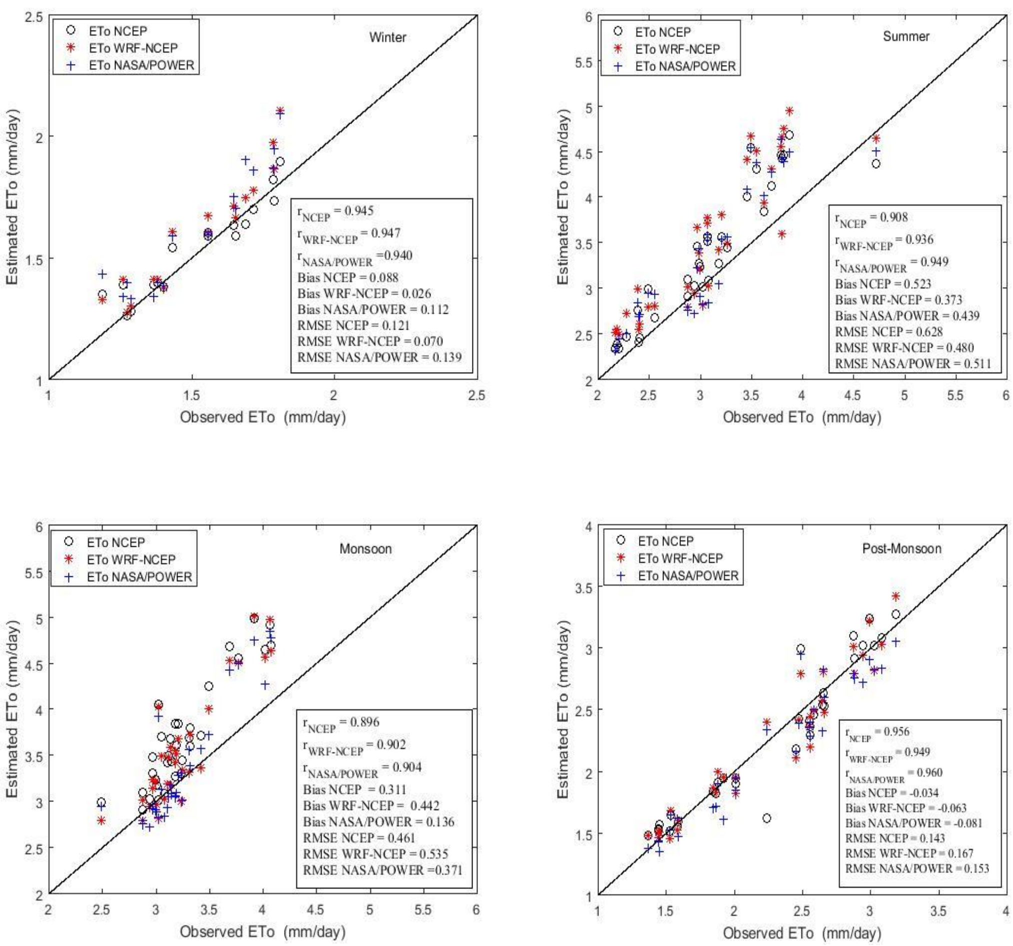

Figure 9. **Scatter plots representing seasonal variations in ETo estimated from NCEP, WRF-NCEP, NASA/POWER and observed data.**

Table 2. Performance statistics for the seasonal and pooled daily ETo

ETo	NCEP			WRF-NCEP			NASA/POWER		
	r	*RMSE*	*Bias*	*r*	*RMSE*	*Bias*	*r*	*RMSE*	*Bias*
Pooled	0.959	0.422	0.241	0.969	0.402	0.230	0.960	0.348	0.154

Winter	0.945	0.121	0.089	0.947	0.070	0.026	0.940	0.139	0.112
Summer	0.908	0.628	0.523	0.936	0.480	0.373	0.949	0.511	0.439
Monsoon	0.896	0.461	0.311	0.902	0.535	0.442	0.904	0.373	0.136
Post- Monsoon	0.956	0.143	-0.034	0.949	0.167	-0.063	0.960	0.153	-0.081

3.5 Comparison with the Penman Monteith estimated ETo

For calculation of ETo using the Penman Monteith method, the dataset of wind speed, solar radiation, relative humidity and air temperature were taken into account, obtained from the ground based meteorological station. Penman Monteith method is now globally accepted method for calculation of ETo and can be used here to check the performances of different ETo products. The ETo obtained from Penman Monteith method is used as benchmark to evaluate the results of the WRF-NCEP, NASA/POWER and NCEP based ETo calculated using the Hamon's method and the results are shown through the Taylor diagram (Fig.10). Taylor diagram is an integrated way of showing the performances in terms of correlation, deviation and RMSE using a single diagram. The circle mask in the x-axis is the reference point, represent the ETo estimated from the Penman Monteith's methods, whereas the position of the different labels reflects the statistical characteristics of the different model data with the observed one. In the figure, it showed that the NASA/POWER has maximum agreement with the observed data in terms of correlation, RMSE and deviation followed by WRF-NCEP, and NCEP. Therefore, from the overall performance, the NASA/POWER has shown the skillful results in estimation of ETo over the study area.

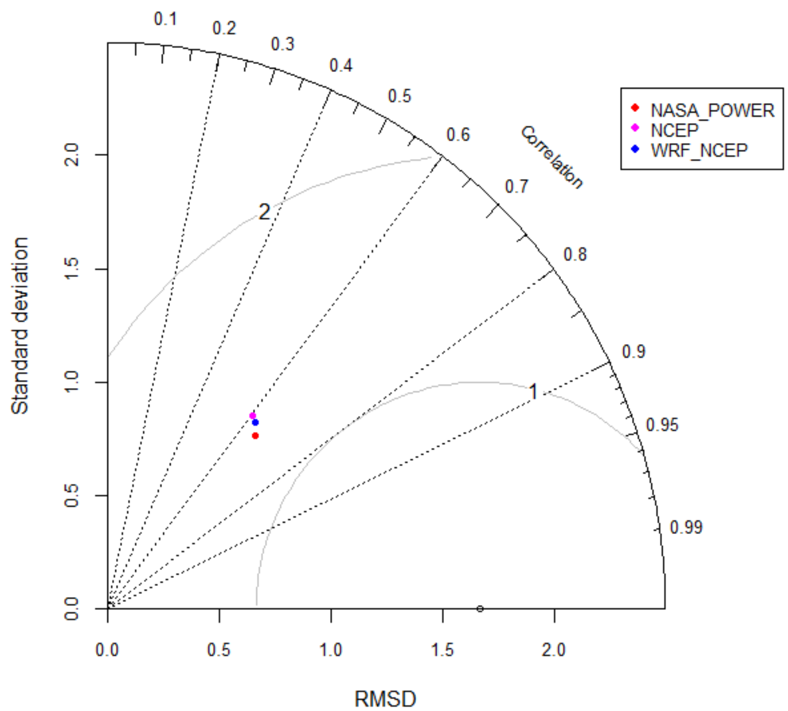

Fig.10 Performance of the NASA_POWER, NCEP and WRF-NCEP estimated ETo with the Penman Monteith based ETo as benchmark

4. Conclusions

Despite the prime importance of evapotranspiration in various hydrometeorological application, it is not often possible to assess evapotranspiration from ground-based weather station. An alternative to this is the use of various reanalysis global datasets and use of mesoscale model for downscaling the global reanalysis data for ungauged sites to estimate ETo. However, there are not many well documented studies available in the literature to show the performance of the NCEP (with WRF downscaling), NASA/POWER for ETo estimation, especially for the Indian regions. In this study, an attempt has been made to evaluate the performance of various global reanalysis datasets and the capability of WRF model in estimating evapotranspiration over an agricultural field. Therefore, this paper provides a detailed cross comparison of ETo estimated from different existing datasets--NCEP, WRF downscaled NCEP and NASA/POWER over cropland by using the Hamon's and Penman Monteith's methods. In order to check the performances of different datasets, the WRF model was used to downscale the global NCEP data into much finer resolution. The accuracy and seasonal performance of ETo estimated from three globally products NCEP global reanalysis and WRF downscaled and NASA/POWER were compared with the ground-based measurements. The temperature variable is used for the estimation of ETo using the Hamon's method on both annual and seasonal basis. Based on the results, the NASA/POWER and WRF-NCEP estimated ETo using Hamon's method is giving accurate result and showed a close match with the ground-based dataset. The ETo values calculated using the different datasets and Hamon's method were compared against the Penman-Monteith method as well, which also showed a close agreement of the ETo calculated from different global dataset with the observed one. Overall, the NASA/POWER showed a close agreement with the observed dataset in terms of Bias and RMSE, which indicates that the NASA/POWER is good to use for different applications as it needs less calculation in comparison to WRF that needs sophisticated schemes and require high power computing system. The outcomes of the study could be helpful in assessing the reliability of the NCEP, WRF downscaled NCEP and NASA/POWER data for various hydrometeorological applications. Further, this study can improve forecasting application and effectiveness of hydro-meteorological modelling especially for the ungauged areas.

Acknowledgement

The authors would like to thank the SERB-DST for funding this research and DST-Mahamana Centre for Excellence in Climate Change Research, Institute of Environment and Sustainable Development, Banaras Hindu University, for providing necessary support for this research. The authors would like to thank the National Centers for Environmental Prediction for providing the NCEP data and NASA Langley Research Center (LaRC) POWER Project for providing NASA-POWER datasets. The authors are also thankful to the Institute of Agricultural Sciences, Banaras Hindu University for providing ground based observational datasets.

References

http://imd.gov.in/section/nhac/wxfaq.pdf

Alkaeed O, Flores C, Jinno K, Tsutsumi A (2006) Comparison of several reference evapotranspiration methods for Itoshima Peninsula area, Fukuoka, Japan Memoirs of the Faculty of Engineering, Kyushu University 66:1-14

Allen RG, Pereira LS, Raes D, Smith M (1998) Crop evapotranspiration-Guidelines for computing crop water requirements-FAO Irrigation and drainage paper 56 Fao, Rome 300:D05109

Cai J, Liu Y, Lei T, Pereira LS (2007) Estimating reference evapotranspiration with the FAO Penman–Monteith equation using daily weather forecast messages Agricultural and Forest Meteorology 145:22-35

Cai X, Wang D, Laurent R (2009) Impact of climate change on crop yield: a case study of rainfed corn in central Illinois Journal of Applied Meteorology and Climatology 48:1868-1881

Chen D, Gao G, Xu C-Y, Guo J, Ren G (2005) Comparison of the Thornthwaite method and pan data with the standard Penman-Monteith estimates of reference evapotranspiration in China Climate Research 28:123-132

Djaman K et al. (2015) Evaluation of sixteen reference evapotranspiration methods under sahelian conditions in the Senegal River Valley Journal of Hydrology: regional studies 3:139-159

Dudhia J (1988) Numerical Study of Convection Observed during the Winter Monsoon Experiment Using a Mesoscale Two-Dimensional Model Journal of the Atmospheric Sciences 46:3077-3107 doi:10.1175/1520-0469(1989)046<3077:NSOCOD>2.0.CO;2

Falk M et al. (2014) Evaluated crop evapotranspiration over a region of irrigated orchards with the improved ACASA–WRF model Journal of Hydrometeorology 15:744-758

Hamon WR (1960) Estimating potential evapotranspiration. Massachusetts Institute of Technology

Hong S-Y, Lim J-OJ (2006) The WRF single-moment 6-class microphysics scheme (WSM6) J Korean Meteor Soc 42:129-151

Ishak AM, Bray M, Remesan R, Han D (2010) Estimating reference evapotranspiration using numerical weather modelling Hydrological processes 24:3490-3509

Kalnay E et al. (1996) The NCEP/NCAR 40-year reanalysis project Bulletin of the American meteorological Society 77:437-472

Kar SK, Nema A, Singh A, Sinha B, Mishra C (2016) Comparative study of reference evapotranspiration estimation methods including Artificial Neural Network for dry sub-humid agro-ecological region Journal of Soil and Water Conservation 15:233-241

Kim H-J, Wang B (2011) Sensitivity of the WRF model simulation of the East Asian summer monsoon in 1993 to shortwave radiation schemes and ozone absorption Asia-Pacific Journal of Atmospheric Sciences 47:167-180

Lang D et al. (2017) A Comparative Study of Potential Evapotranspiration Estimation by Eight Methods with FAO Penman–Monteith Method in Southwestern China Water 9:734

Lin P et al. (2018) Spatiotemporal Evaluation of Simulated Evapotranspiration and Streamflow over Texas Using the WRF-Hydro-RAPID Modeling Framework JAWRA Journal of the American Water Resources Association 54:40-54

Mall R, Gupta B (2002) Comparison of evapotranspiration models Mausam 53:119-126

McCabe GJ, Hay LE, Bock A, Markstrom SL, Atkinson RD (2015) Inter-annual and spatial variability of Hamon potential evapotranspiration model coefficients Journal of Hydrology 521:389-394

Mlawer EJ, Taubman SJ, Brown PD, Iacono MJ, Clough SA (1997) Radiative transfer for inhomogeneous atmospheres: RRTM, a validated correlated-k model for the longwave Journal of Geophysical Research: Atmospheres 102:16663-16682

Mohan M, Sati AP (2016) WRF model performance analysis for a suite of simulation design Atmospheric Research 169:280-291

Monteith J (1965) Evaporation and environment. pp. 205-234. In GE Fogg Symposium of the Society for Experimental Biology The State and Movement of Water in Living Organisms 19

Nag A, Adamala S, Raghuwanshi N, Singh R, Bandyopadhyay A (2014) Estimation and Ranking of Reference Evapotranspiration for Different Spatial Scale in India vol 34.

Pandey PK, Dabral PP, Pandey V (2016) Evaluation of reference evapotranspiration methods for the northeastern region of India International Soil and Water Conservation Research 4:52-63

Penman H (1956) Estimating evaporation: Transactions Am Geophys Union 39:19-56

Petropoulos G, Ireland G, Cass A, Srivastava P (2015) Performance Assessment of the SEVIRI Evapotranspiration Operational Product: Results Over Diverse Mediterranean Ecosystems IEEE Sensors DOI:101109/jsen20152390031

Petropoulos GP et al. (2016) Operational evapotranspiration estimates from SEVIRI in support of sustainable water management International Journal of Applied Earth Observation and Geoinformation 49:175-187

Podder S, Khan RS, Mohon SMAA, Hussain MJ, Basher E Solar radiation approximation using sunshine hour at patenga, Bangladesh. In: Electrical and Computer Engineering (ICECE), 2014 International Conference on, 2014. IEEE, pp 321-324

Schwartz CS et al. (2009) Next-day convection-allowing WRF model guidance: A second look at 2-km versus 4-km grid spacing Monthly Weather Review 137:3351-3372

Silva D, Meza FJ, Varas E (2010) Estimating reference evapotranspiration (ETo) using numerical weather forecast data in central Chile Journal of hydrology 382:64-71

Skamarock WC, Klemp JB, Dudhia J Prototypes for the WRF (Weather Research and Forecasting) model. In: Preprints, Ninth Conf. Mesoscale Processes, J11–J15, Amer. Meteorol. Soc., Fort Lauderdale, FL, 2001.

Srivastava PK, Han D, Islam T, Petropoulos GP, Gupta M, Dai Q (2016) Seasonal evaluation of evapotranspiration fluxes from MODIS satellite and mesoscale model downscaled global reanalysis datasets Theoretical and Applied Climatology 124:461-473

Srivastava PK, Han D, Rico Ramirez MA, Islam T (2013) Comparative assessment of evapotranspiration derived from NCEP and ECMWF global datasets through Weather Research and Forecasting model Atmospheric Science Letters 14:118-125

Srivastava PK, Han D, Yaduvanshi A, Petropoulos GP, Singh SK, Mall RK, Prasad R (2017) Reference Evapotranspiration Retrievals from a Mesoscale Model Based Weather Variables for Soil Moisture Deficit Estimation Sustainability 9:1971

Thornthwaite CW (1948) An Approach toward a Rational Classification of Climate Geographical Review 38:55-94 doi:10.2307/210739

Zotarelli L, Dukes MD, Romero CC, Migliaccio KW, Morgan KT (2010) Step by step calculation of the Penman-Monteith Evapotranspiration (FAO-56 Method) Institute of Food and Agricultural Sciences University of Florida